We are IntechOpen, the world's leading publisher of Open Access books Built by scientists, for scientists

6,900
Open access books available

185,000
International authors and editors

200M
Downloads

Our authors are among the

154
Countries delivered to

TOP 1%
most cited scientists

12.2%
Contributors from top 500 universities



WEB OF SCIENCE™

Selection of our books indexed in the Book Citation Index in Web of Science™ Core Collection (BKCI)

Interested in publishing with us?
Contact book.department@intechopen.com

Numbers displayed above are based on latest data collected.
For more information visit www.intechopen.com



Chapter

Dissimilar Welding and Joining of Magnesium Alloys: Principles and Application

Kavian O. Cooke, Abdulaziz Alhazaa and Anas M. Atieh

Abstract

The growing concerns regarding fuel consumption within the aerospace and transportation industries make the development of fuel-efficient systems a significant engineering challenge. Currently, materials are selected because of their abilities to satisfy engineering demands for good thermal conductivity, strength-to-weight ratio, and tensile strength. These properties make magnesium an excellent option for various industrial or biomedical applications, given that is the lightest structural metal available. The utilization of magnesium alloys, however, requires suitable welding and joining processes that minimizes microstructural changes while maintaining good joint/bond strength. Currently, magnesium are joined using; mechanical fastening, adhesive bonding, brazing, fusion welding processes or diffusion bonding process. Fusion welding is the conventional process used for joining similar metals. However, the application of any welding technique to join dissimilar metals presents additional difficulties, the principal one being; the reaction of the two metals at the joint interface can create intermetallic compounds that may have unfavorable properties and metallurgical disruptions which deteriorates the joint performance. This chapter investigates the welding and joining technologies that are currently used to join magnesium alloys with emphasis on the development of multi-material structures for applications in the biomedical industries. Multi-material structures often provide the most efficient design solution to engineering challenges.

Keywords: magnesium, solid-state diffusion bonding, friction stir welding, dissimilar joining, transient liquid phase

1. Introduction

The interest in the use of lightweight materials and alloys has significantly increased in recent years due to excellent mechanical and chemical characteristics; such as high specific strength, low weight, and corrosion resistance. Magnesium is a popular industrial metal and it is the lightest of all, estimated to be 33% lighter than aluminum and ~75% lighter than steel, with a density of 1.74 g/m^3 [1]. Magnesium has a hexagonal closed pack (HCP) crystalline structure that resists the slip to parallel basal planes and therefore, magnesium cannot be plastically deformed at room temperature, because the work hardening rate is high, and ductility is low. Therefore, magnesium alloys are formed above 226°C with a range of 343–510°C as

the slip process becomes easier at elevated temperatures. Anisotropy during deformation is the other consequence of the HCP structure in cold-formed sheets.

The industrial and biomedical demand for components made from light-weight materials have only increased over the last decade [1]. In its pure state, magnesium is ductile and possesses low tensile strength in the range of 20 MPa. Engineering applications, however, require greater strength as such magnesium if frequently alloyed with elements such as; Al, Mn, Zn, Li, Ag, Ca and Cu along with various minor alloying elements. The utilization of magnesium alloys has seen an increase at the rate of 15% and is predicted to go even higher over the next decade. Currently, magnesium is used widely as a structural material due to low density and favorable damping characteristics, low casting costs and machinability [2]. However, new magnesium alloys are being developed with enhanced corrosion resistance and enable these materials to operate satisfactorily inside the human body. The corrosion resistance of these materials has been shown to be inversely proportional to the volume of impurity (Fe, Ni, and Cu) present in the alloy. Currently, the high purity ZX50 Mg alloy and high purity Mg-Al alloys have shown the greatest degree of success.

A major challenge in using these materials is the unavailability of suitable welding technique capable of both similar and dissimilar welding of magnesium alloys [3]. Currently, magnesium alloys used in dissimilar welding processes are joined by resistance spot welding, laser welding, friction stir welding, and diffusion bonding. Extensive research has been devoted to the development of technologies capable of joining these alloys while preventing significant microstructural changes commonly observed during fusion welding of advanced composites. This chapter will investigate welding and joining technologies which are currently used to join magnesium alloys with emphasis on diffusion bonding as a technique for the development of multi-material structures for applications in the biomedical industries. Multi-material structures often provide the most efficient design solution to engineering challenges. The use of several metals in the construction of multi-material structures is limited by the ability of the available welding/joining technologies to join dissimilar materials together.

2. Welding metallurgy of magnesium alloys

Fusion welding of magnesium alloys has been studied using several technologies which include; gas tungsten arc welding (TIG), gas metal arc welding (MIG), laser welding and ultrasonic welding. During TIG welding, an arc is produced between a non-consumable electrode and the workpiece, which melts the base metal to form a weld/joint as shown in **Figure 1**. The joint and surrounding areas can be divided into regions consisting of the weld pool (with a cast structure) and a heat affected zone (HAZ). The microstructural changes within these regions occur due to the temperature gradient from the weld pool to the base metal alloy as shown in **Figure 2**. Shielding flux either in solid or gaseous form is required to protect the weld pool from exposure to oxygen.

TIG welding is considered as the most preferred industrial welding method for reactive materials such as magnesium; this is attributed to better economy and applicability, which makes it an excellent choice for joining magnesium and its alloys. Previous work on joining Mg alloys showed that TIG welding may result in a joint strength of up to 94% of the shear strength of the Mg base metal alloy. However, grain size variation from 6 to 23 μm occurred, across the weld pool, heat affected zone (HAZ) region, and Mg base metal alloy, when TIG welding is applied without a filler wire [4]. On the other hand, Peng et al. [5] showed that dissimilar joining of magnesium alloys AZ31 and AZ61 using TIG welding can

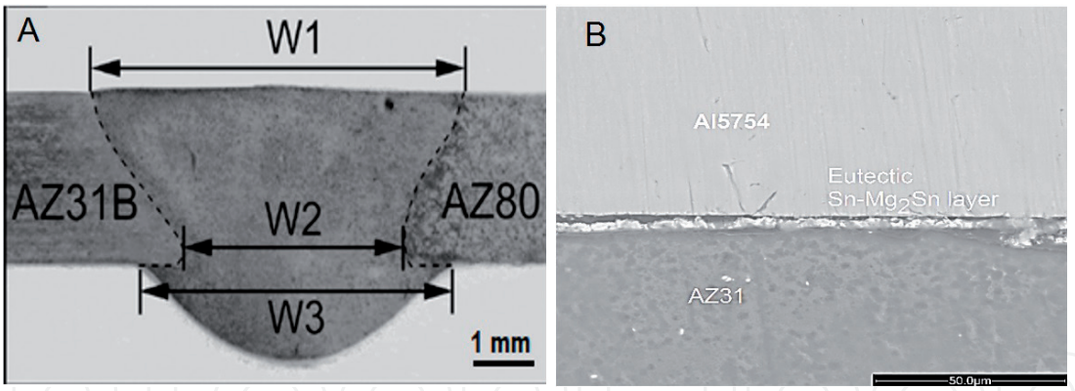


Figure 1.
Micrographs showing the transverse section of joint welded by (a) TIG welding (b) ultrasonic welding [4].

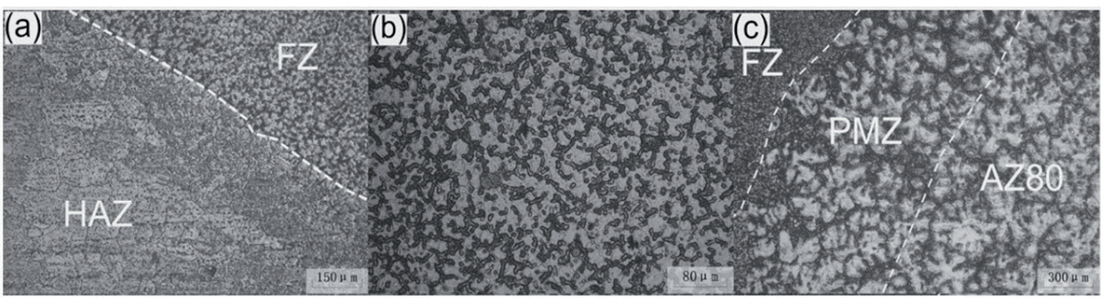


Figure 2.
Microstructures of the welding joint produced by TIG welding (a) AZ31 side of the weld; (b) fusion zone; (c) AZ80 side of the weld [4].

achieve a bond strength of 84%. In their recent work, Song et al. [4] also showed that laser TIG welding produced good weldability and joint strength in Mg alloys when compared with hybrid welding. The hybrid welding approach resulted in a more flexible and reliable methodology for industrial application for magnesium alloys welding. The increased joint strength of Mg-AZ31 joints produced by hybrid TIG welding was attributed to the formation of a partially melted zone (PMZ) [4]. Several researchers successfully achieved dissimilar joining of magnesium alloys. The results of these studies demonstrated that while it is possible to join magnesium using TIG welding the heat input during welding results in significant changes in the HAZ that limits the strength of the joints produced. **Figure 2** shows an optical micrograph of fusion zone and the heat affected zone (HAZ) for two types of magnesium alloys joined using TIG welding, while the chemistry of the materials is different, the microstructural changes within the FZ and HAZ are similar in both alloys [4, 6].

Similarly, MIG welding has been shown by several researchers to be capable of joining magnesium alloys with greater speed when compared to TIG welding. Unique fast rigging proportions are normally required in the wire feeders since the magnesium terminal wire has a high melt-off rate. The typical wire feeder and power supply utilized for aluminum welding will be appropriate for welding magnesium. The heat input during MIG welding of magnesium alloys, however, results in the formation of a large HAZ containing a coarse grain structure which lowers the mechanical performance of the weld [7].

Recent studies in resistance spot welding (RSW) of magnesium alloys have demonstrated that dissimilar RSW of magnesium AZ31 to aluminum Al5754 coated with nanostructured electrodeposited coating prevented intermetallic formation while enhancing joint strength. RSW is the most common welding technique used in the

automotive industry because it is inexpensive, easily automated, and capable of producing high-quality welds [8]. The process is based on the contact resistance between the metals to be joined and the electrodes [9]. During the process, a weld nugget is formed by the melting of the materials as the temperature increases due to the materials' resistance. The heat generated during resistance spot welding (RSW) is based on Joule's law. However, the presence of surface oxides on magnesium alloys necessitates the use of high welding current because of the high contact resistance which also leads to rapid erosion of electrode tips used in the welding process. The scientific literature, however, shows that the heat input by RSW dissimilar joining of Al-Mg alloys leads to the formation of $Al_{12}Mg_{17}$ and Al_3Mg_2 intermetallic compounds within the weld nugget [10–12]. A recent study using Ni/TiO_2 interlayer showed that the intermetallic formation during dissimilar resistance spot welding of magnesium to aluminum can be controlled with the inclusion of nanoparticles at the interface (see **Figure 3**) however, the addition of a coating step in the process extends the process time [13]. Despite the advancements that have been made regarding the impact of interlayers such as Zn as an interlayer between Al/Mg alloys, gold coated Ni interlayer [14, 15] and adhesive interlayers [16], to enhance the mechanical properties of the joints.

Laser welding, on the other hand, permits dissimilar joining of magnesium alloys while limiting the width of the HAZ, due to a smaller diameter beam and greater control of power input. However, the equipment used for laser welding is expensive and requires skilled operators. Furthermore, laser welding is usually applied to delicate and thin sheets due to the low penetration of laser beam into the materials. Ultrasonic spot welding (USW) have also been shown to eliminate some of the challenges encountered during RSW since the amount energy input into the material during welding is significantly lower, typically in the range of 0.5–1.2 kJ and requires a shorter welding time [17]. **Figure 1(B)** shows the microstructure of a bond made by ultrasonic welding. The formation of Mg_2Sn layer at the interface has been shown to limit the mechanical strength of the weld.

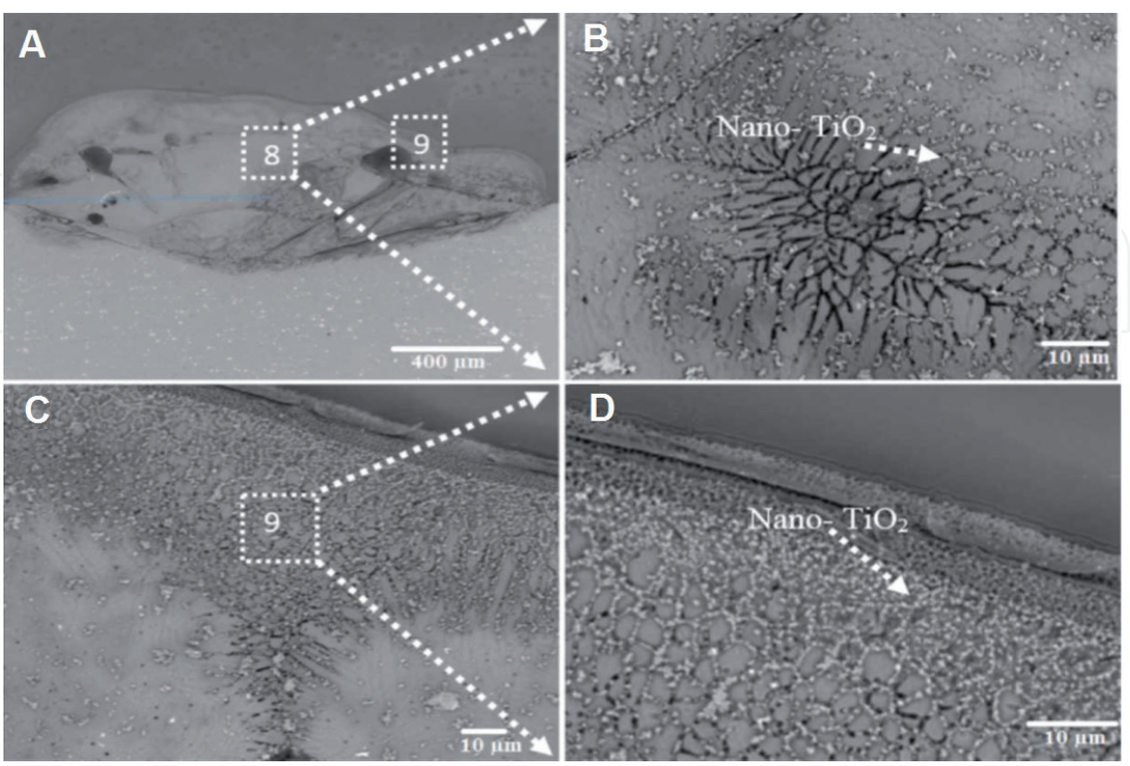


Figure 3.
SEM micrograph showing: (A) Al/Ni–TiO_2/Mg spot weld, (B) microstructure of point-8, (C) Al/weld nugget interface and (D) microstructure of point-9 [13].

A major challenge in welding magnesium alloys, however, is the presence of a surface oxide. Magnesium has a relatively low melting point, however, the surface oxide has a high melting point, as such removal of the surface oxide is required before welding of the metal. Additionally, several quality issues have been shown to arise during fusion welding of magnesium alloys. For example; large shrinkage during solidification and high chemical reactivity of Mg makes it very difficult to weld using traditional welding techniques [18], hence, Mg is usually alloyed with aluminum, zinc, and manganese for commercial usage [18]. A critical consideration is necessary for welding Mg alloys that may be affected by the properties of the alloying elements [19]. Any oxygen in contact with the weld pool, regardless of whether from the climate or the protecting gas, causes dross. Therefore, an adequate stream of idle protecting gases is essential, and welding in moving air ought to be avoided.

While fusion welding has been successfully used for similar metal joining of magnesium alloys, dissimilar welding of magnesium alloys to metals such as: steel [20], aluminum [21], and titanium has significant limitations due to the formation of intermetallic compounds within the joint region that minimize the joint strength and limits its potential applications. The formation of various Mg-Al intermetallic compounds is detrimental to the mechanical performance of the materials. The formation of these compounds can be minimized with the use of interlayers between the materials to be joined. Given the potential for intermetallic formation, various joining techniques have been extensively studied with the objective being to minimize the formation of intermetallic compounds during joining while improving joint performance. Some of these techniques include friction stir welding, resistance spot welding, laser welding, ultrasonic welding, and diffusion bonding. These limitations have led to a preference for solid-state joining techniques to weld/join Mg and its alloys to other metals.

3. Friction stir welding

Friction stir welding (FSW) is a solid-state welding process that was developed at The Welding Institute (TWI) [22]. As explained by Mishra and Ma, the process is carried out by the use of a non-consumable rotating pin which travels along the joint to be welded [23]. The friction between the tool and the materials generates heat which softens the material [24]. **Figure 4** shows a schematic of the FSW

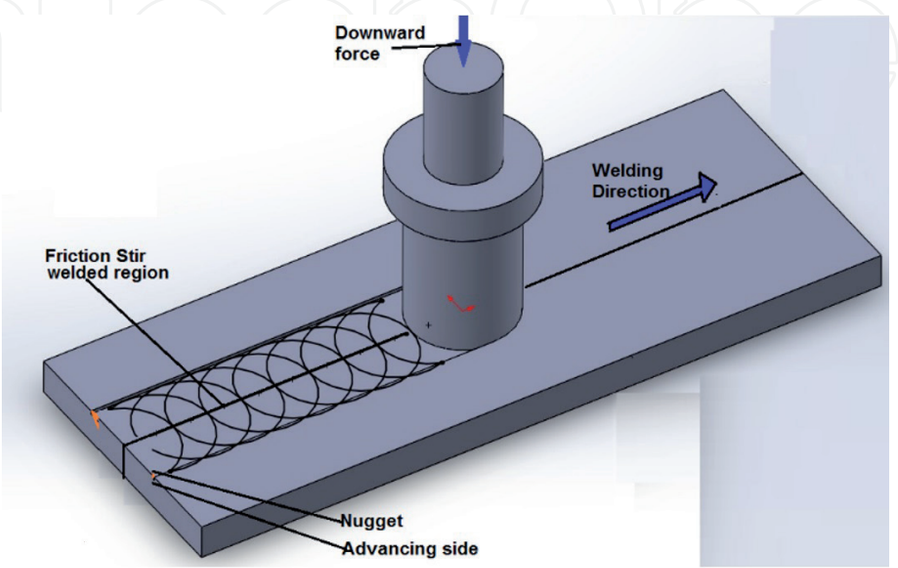


Figure 4.
Schematic of the friction stir welding process.

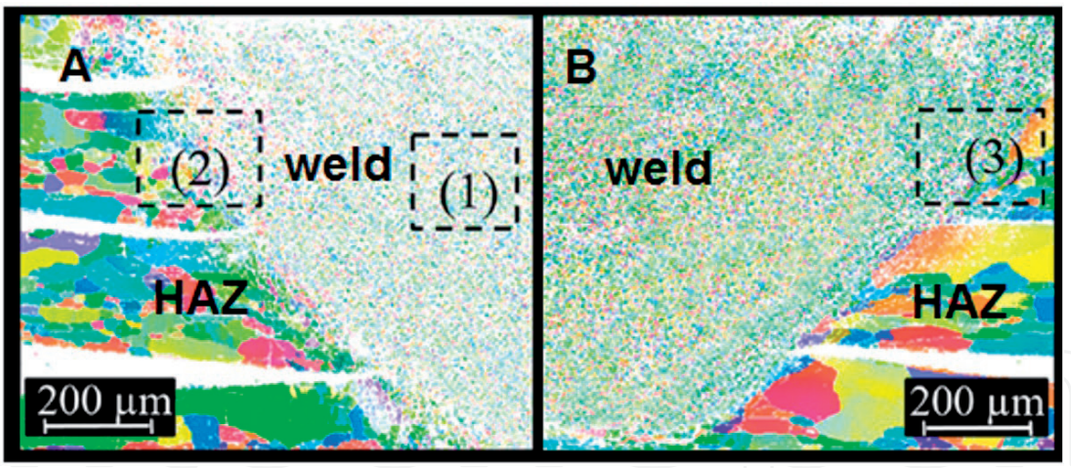


Figure 5.
Weld produced by friction stir welding and the microstructure generated [26].

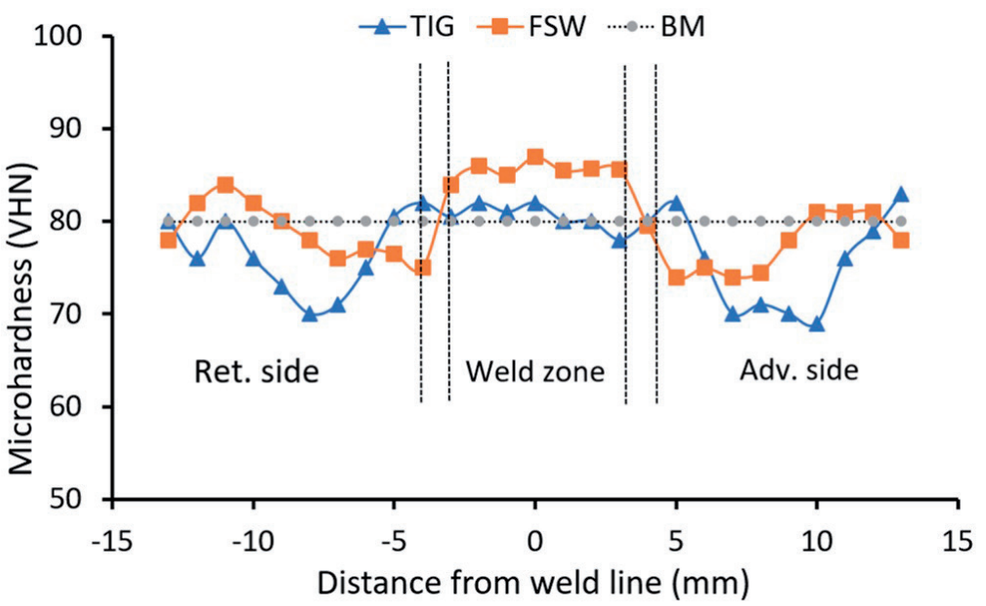


Figure 6.
Hardness profiles across Mg-alloys welded using friction stir welding and TIG welding.

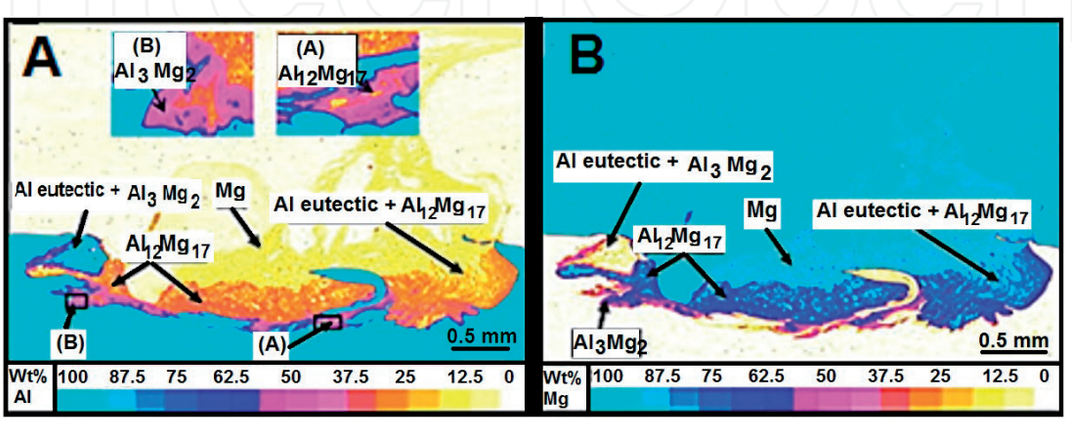


Figure 7.
EPMA results of the FSW region of the sample welded by using a weld-pitch ratio of 1400/40 r/mm in the cross-section perpendicular to the tool transverse direction. Element distribution: (A) Al and (B) Mg [36].

process. The combination of tool rotation and localized softening of the material causes movement of the material leading to a weld. The process was first developed to weld aluminum alloys [22] previously described as non-weldable because of the adverse solidification microstructural formed in the fusion zone during fusion welding. Since its development, however, the technology has been applied to various metal and alloys. Zhang [25] demonstrated that friction stir welding is a viable technique for joining magnesium alloys.

Mg joints produced by FSW are characterized by high joint strength, high fatigue resistance, less distortion, since consumables are not required hence it is cheaper and no loss of alloying elements occurs during the process [27, 28].

The literature shows that weld quality is dependent on the optimization of the welding parameters; tool shape, jig rotational speed, tool speed, and joint configuration. In comparison to the traditional welding zones, the weld produced by FSW was characterized by four distinct zones as shown in **Figure 5** [26, 29]. These regions include; stirring zone (SZ), thermo-mechanical affected zone (TMAZ), heat affected zone (HAZ), and base metal (BM) [26, 30]. Singh et al. [23] demonstrated that FSW is capable of Mg weld with shear strength ranging from 66 to 410 MPa and the hardness from 50 to 110 HVN which represents 60–195% joint efficiency compared to the base metal alloy. **Figure 6** shows the hardness variation across the weld and confirms the hardness variations reported by Singh et al. The difference between the hardness recorded at the center of the weld and the base metal was attributed to the formation of IMCs with the weld during the FSW process. Similar findings were recorded by other researchers who studied different Mg alloys were welded using FSW such as; MgAZ31 [31, 32] and MgAZ31B [33], dissimilar joint of Al6061/MgAZ31B [34, 35]. Mohammadi et al. [36] demonstrated that while FSW can reduce the volume of intermetallic compounds formed during dissimilar welding, some IMCs will still form as shown in **Figure 7**.

4. Diffusion bonding

Diffusion bonding is a non-conventional solid-state welding process that can join a variety of materials in the solid state below the melting point of the base materials. The core mechanism involves the interdiffusion of atoms between the faying surfaces at the interface [37]. The process is frequently completed by one of two methods; firstly, solid-state diffusion bonding in which the base metals to be joined are heated to approximately 60% of the melting temperature of the metals under the influence of static load. Melting at the interface of the faying surfaces is prevented, however, interdiffusion of the diffusing species leads to the formation of solid-state bond. The second method is referred to as a transient liquid phase (TLP) diffusion bonding in which an interlayer is placed between the metals to be joined. Interdiffusion between the interlayer and the base metals facilitates the formation of a eutectic reaction which transitions from liquid to solid by isothermal solidification as the composition of the eutectic liquid changes due to diffusion. Each method will be further discussed below. A schematic of the diffusion bonding process is shown in **Figure 8**.

4.1 Solid-state diffusion bonding of magnesium alloys

Solid state diffusion bonding occurs due to the migration of atoms at the interface of the materials to be joined. The faying surfaces do not undergo any metallurgical discontinuity and as a result, the mechanical and microstructural property

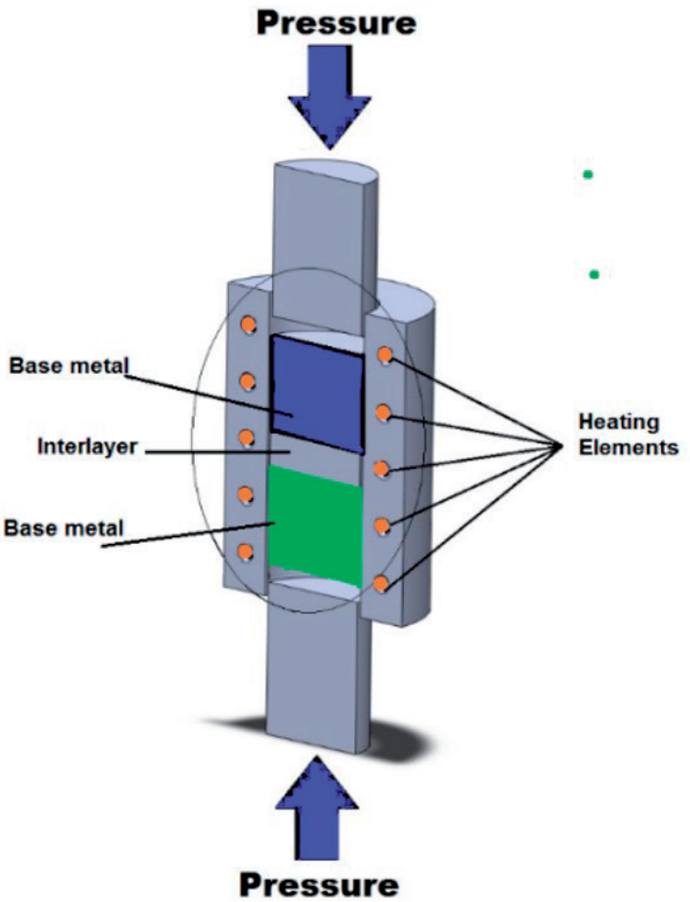


Figure 8.
Schematic of the diffusion bonding process.

of the joint formed closely resembles those of the base materials [38]. Solid-state diffusion bonding goes through three distinct stages. The first stage includes; contact of the faying surfaces. In this stage, removal of surface roughness and irregularity play a significant role in ensuring good contact between the faying surfaces. Secondly, micro-plastic deformations at the interface, as the pressure inside the voids decreases and finally, grain boundary migration that fills the shrinkage and minimizes surface free energy. Surface preparation typically includes generation of a smooth surface and elimination of any oxides from the faying surfaces. Application of the pressure at the first stage ensures a good contact between the faying surfaces. Bonding pressure, temperature, and holding time are critical to achieving good bonds. Eq. (1) shows that the bonding temperature is proportional to the coefficient of the diffusing species. While the applied pressure ensures metal–metal contact and micro-plastic deformation of asperities at the interface of the faying surfaces.

$$D = D_o e^{-\frac{Q}{RT}} \tag{1}$$

Where, D is the diffusion coefficient of the diffusing species, D_o is the pre-exponential term, R is gas constant and T is the bonding temperature. While bonding/hold time can be directly related to the volume of the diffusing species using Fick's second law of diffusion. Increasing the hold time is expected to enhance diffusion and strength the bond.

Diffusion bonding has been studied extensively as a method for both similar and dissimilar joining of magnesium alloys. The high temperature used in fusion welding process leads to the formation of intermetallic compounds, which have been shown to be detrimental to the mechanical performance of the joints when joining

magnesium alloys. Unfortunately, the dissimilar joining of magnesium alloys to other metals is significantly inhibited by the differences in the properties of the materials such as melting temperature, the coefficient of thermal expansion and thermal conductivity. Solid-state diffusion bonding limits intermetallic formations during dissimilar bonding and maximizes joint strength.

Figure 9 shows the SEM micrograph of a solid-state diffusion bond formed between titanium (Ti-6Al-4V) and magnesium (AZ31) for 60 minutes. The width of the reaction layer at the interface appears to be in the form of dispersed particles approximately 20 μm in length. EDS point analysis of the samples revealed the formation of several compounds at the bond interface. The results show that holding the sample at the bonding temperature, Al reacts with Ti and Mg leading to the precipitation of the $TiAl_3$ and $Ti_2Mg_3Al_{18}$ intermetallic compounds at the Ti interface. The $Mg_{17}Al_{12}$ intermetallic compounds appear to have formed at the Mg grain boundaries. The $Mg_{17}Al_{12}$ compound is believed to have been produced by a eutectic reaction between Al and Mg. The joint formation was attributed to metallurgical bonding driven leading to the formation of $TiAl_3$ and $Ti_2Mg_3Al_{18}$. It is expected that the differences in the melting temperature of the two alloys at the bonding temperature of 500°C will cause the Mg sample to plastically deform ensuring complete contact with the Ti sample. Hidetoshi Somekawa [39] demonstrated that diffusion bonding of superplastic magnesium sheets is heavily dependent on the grain size of the material. For samples with grain size in the range of 11–15 μm bond strength of approximately 92% of the base metal strength is possible. According to the Ti-Mg-Al ternary phase diagram the following phases; Mg_2Al_3, $Mg_{17}Al_{12}$, $TiAl_3$ and $TiAl_2$ are likely to form at the bonding temperature and pressure used in this study [6]. The Gibbs energy for the formation of $TiAl_3$ is approximately 234 kJ/mol, $TiAl_2$ is 237 kJ/mol [40]. The diffusion of Al to the bond interface from Ti-side to the Mg-side led to the formation of a compound having a stoichiometric composition of $Mg_{17}Al_{12}$ where 43.95 wt.% of the compound is Al [41].

The $Mg_{17}Al_{12}$ is an intermetallic compound with a Gibbs free energy of formation of −6 kJ/mol at a temperature range of 700–1000 K. The Gibbs energy of formation increased to −3.9 kJ/mol. From the Gibbs free energy data, the $Mg_{17}Al_{12}$ intermetallic compound is most negative and therefore is expected to form first at the Mg-interface. The Gibbs energy for the formation of the ternary compound $Ti_2Mg_3Al_{18}$ was found to be approximately −15 kJ/mol [42]. The width of the reaction layer that forms at the interface is believed to be time dependent. As such, the layer thickness bears a direct relation with growth kinetics. The average thicknesses of the $TiAl_3$ and $Ti_2Mg_3Al_{18}$ layers and the total intermetallic layer was used to determine the kinetic parameters involved in the diffusion process.

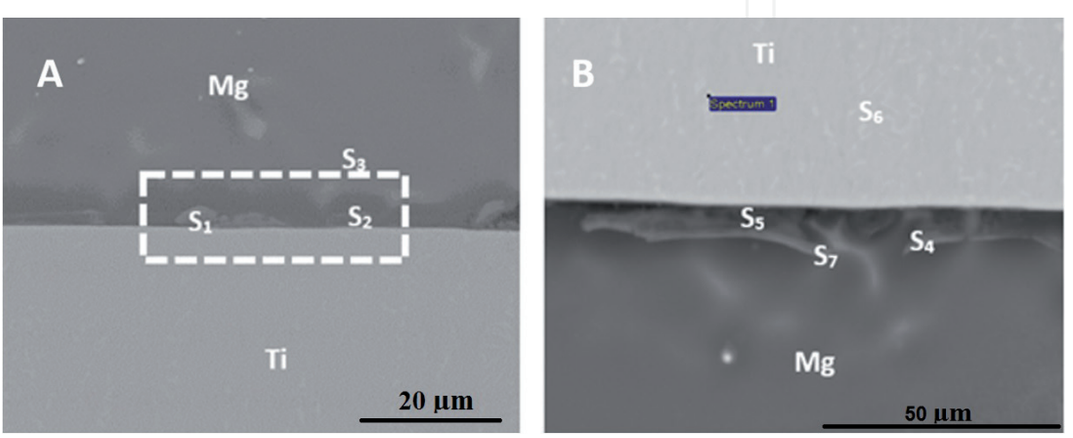


Figure 9.
(A) Solid-state diffusion bonding of Ti and Mg for 60 minutes; (B) magnified region of the bond-line showing the reaction layer at the bond interface;

The data collected shows that as the bonding time increases the width of the reaction layer. The width also increased as predicted by the parabolic law shown in Eq. (2).

$$x = kt^n \tag{2}$$

Where k is the rate factor, t the diffusion time, and n the time exponent. **Figure 10** shows the relationship between the bonding time and the thickness of the reaction layer formed at the interface and shows that as the bonding time increased the thickness of the reaction layer also increased. When the parabolic rate law is applied to the results, the rate coefficient k was calculated to be 15.7×10^{-7} m/s. The value for n was assumed to be 0.5 since the growth of the reaction layer was assumed to be controlled by inter-diffusion. When the calculated rate coefficient is substituted into the parabolic rate law shown in Eq. (1) the results show that the predicted thickness of the intermetallic layer was overestimated by the model.

The difference between the properties of the base metal and the bonded zone was highlighted by the micro-hardness measurements plotted in **Figure 11** as a function of bonding time. The micro-hardness values were measured across the joint starting at 500 μm from the joint center. The figure shows that the hardness of the Ti sample fluctuated between 390 VHN and 420 VHN up to 100 μm from the joint center as the bonding time was increased from 10 to 60 minutes. The hardness within the joint center was observed to decrease to between 190VHN at 10 minutes bonding time and 250 VHN at 60 minutes bonding time. The hardness of the Mg sample was found to be significantly lower than that of the Ti sample with a hardness ranging from 60 VHN at 10 minutes bonding time to 65 VHN. The variation of the hardness number across the interface was attributed to the differences between the properties of Ti and Mg. The hardness at the center of the bond is believed to have been caused by the formation of the reaction layer at the joint interface [43]. The reaction layer was shown to be made-up of $TiAl_3$ and $Ti_2Mg_3Al_{18}$ intermetallic compounds dispersed within the joint region.

4.2 Transient liquid phase diffusion bonding

The transient liquid phase diffusion bonding process occurs due to the formation of a eutectic liquid at the interface between the faying surfaces. The eutectic reaction may form due to interdiffusion between the base metals or an interlayer and base metals which leads to the formation of a eutectic composition. Alternatively, a

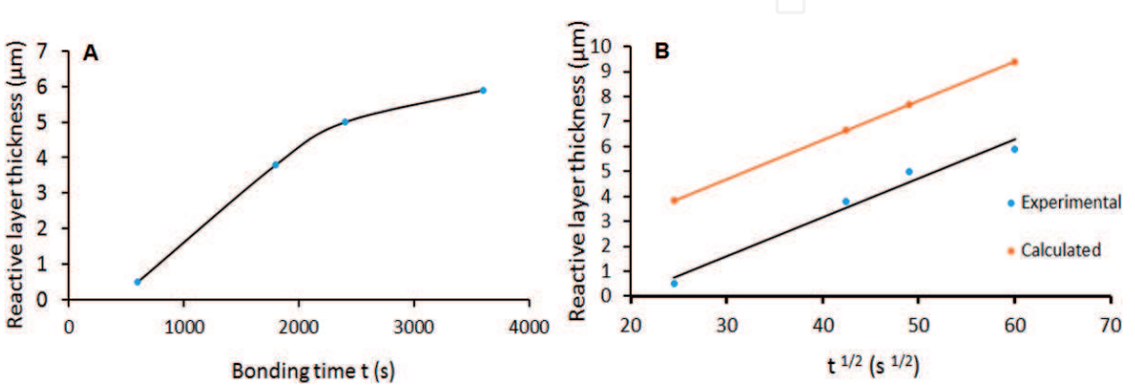


Figure 10.
(A) Shows the relationship between the thickness of the reaction layer and the bonding time; (B) shows the predicted relationship between the thickness of the reaction layer and the bonding time according to the parabolic rate law.

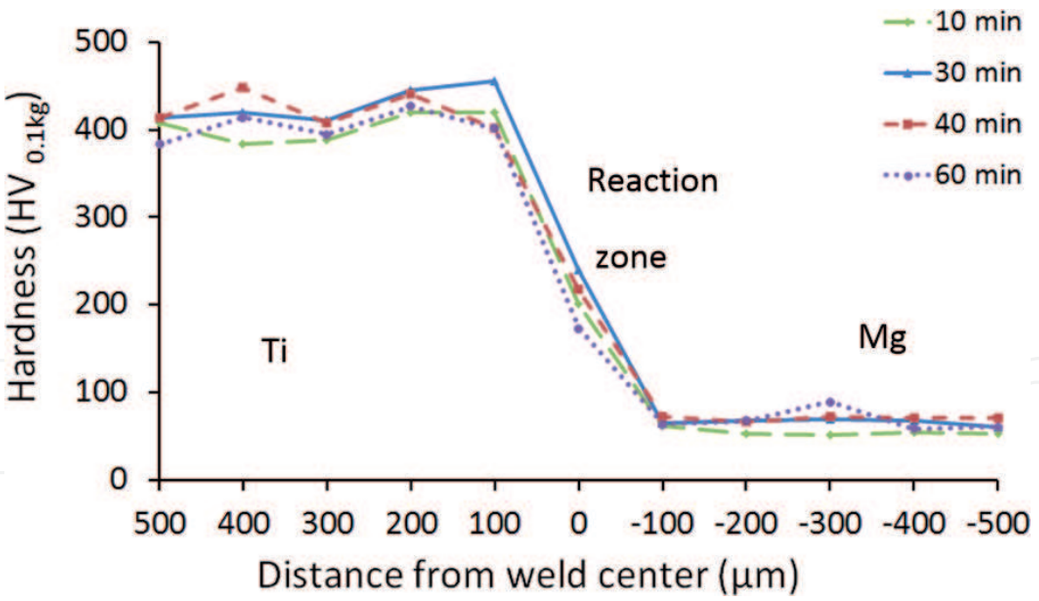


Figure 11.
Micro-hardness measurements across the joint region as a function of bonding time.

thin interlayer having a eutectic composition and melts at the bonding temperature. The formation of the liquid displaces the surface oxides at the bond interface and reduces the bonding pressure requirement normally used to achieve surface contact during solid-state diffusion bonding. The advantage of the process is the potential for minimizing microstructural changes and intermetallic formations within the bond region and achieving joints with higher strength. However, TLP bonding can be a lengthy process that required four distinct stages (heating, dissolution and widen, isothermal solidification and homogenization) for completion [44]. Important parameters studied in TLP bonding include; interlayer composition and thickness, bonding temperature and bonding time [45].

4.2.1 Interlayer thickness and composition

During TLP bonding the thickness and composition of the interlayer used are critical to the volume of liquid formed during bonding and invariably affects the quality of the bonds produced [46]. The scientific literature shows that suitable interlayers must allow eutectic melting while limiting the volume of the liquid that forms in order to control the width of the interface and shorten the homogenization stage of bonding [3]. Additionally, the wettability of the base metals by the molten interlayer is critical to displacing surface oxides in order to form a joint [2]. When suitable interlayers are used, the formation of intermetallic compounds (IMC) can be prevented or significantly reduced. The interlayers can be used in the form of; thin foils, fine powder, compact powder or paste, electroplated and vapor deposited coatings [47].

Selection of the interlayer composition depends on the base materials being joined. The literature shows that materials such as Sn, Ag, Al, Cu, Ni, Cr, V, and Zn are frequently used as interlayers during diffusion bonding. Most commonly used interlayers when joining magnesium alloys include Al, Cu, and Ni since these materials' leads to a eutectic reaction with magnesium which lowers the bonding temperature and catalyzes diffusion. When Al interlayer was used by Sun et al. [3] to bond Mg alloy MgAZ31, brittle IMC, $CuMg_2$ was formed at the joint interface. However, increasing bonding temperature slightly increased the strength of the bond, as a result of microstructure homogenization for short bonding time. When the bonding time was increased beyond 60 minutes grain coarsening occurred which resulted in a reduction in joint strength.

In another study, Jin and Khan [48] studied the use of Ni, as an interlayer while joining the same Mg alloy, and found that the hardness of the joint increased as the bonding time increased as a result of the formation of Mg-Ni IMCs. Research results presented by Alhazaa et al. [49] showed that an optimum bonding time of 20 minutes was attained when bonding Mg AZ31 using Sn coatings. As shown in **Figure 12**, as the bonding time increased the bond line completely disappears, which is an indication of the homogenization of the bond region. The EPMA map shown in **Figure 13**, confirms the diffusion of Sn away from the interface and the homogenization of the composition within the joint region. Nevertheless, the formation of IMC at the joint consequently reduced the bond strength (see **Figure 15**). In contrast, Sun et al. [3] used Cu interlayer and suggested a bonding time of 30 minutes was optimal. The study also showed that the volume of intermetallic compounds formed was inversely proportional to hold time.

The potential for the dissimilar joining of Mg alloys to other metals is significantly greater with TLP bonding. Zhang et al. [50] demonstrated that Ni-coating can be used as an interlayer to join Mg to Al however suitable optimization of the bonding parameters are required to prevent the formation of a Mg_2 Ni IMCs reaction layer between the metals. Alhazaa et al. [51] observed that the application of Cu coatings and Sn interlayers while bonding Mg AZ31 to the Ti-6Al-4V alloy. Increasing the bonding time also decreased the thickness of the IMC Mg_2Cu compounds and better bonds were formed between these dissimilar metal alloys (see **Figure 14**). The use of nanoparticle-reinforced composite interlayer during TLP process has also gained interest recently as they reduce grain size within the bond region and increase joint strength [52]. Similarly, Atieh and Khan [53], showed that when Ti-6Al-4V and Mg-AZ31 alloys were bonded using Ni and Cu nanoparticles, the joint formation was enhanced by increasing the rate of isothermal solidification during the TLP bonding process. **Figure 15** shows a TLP bond that was made between

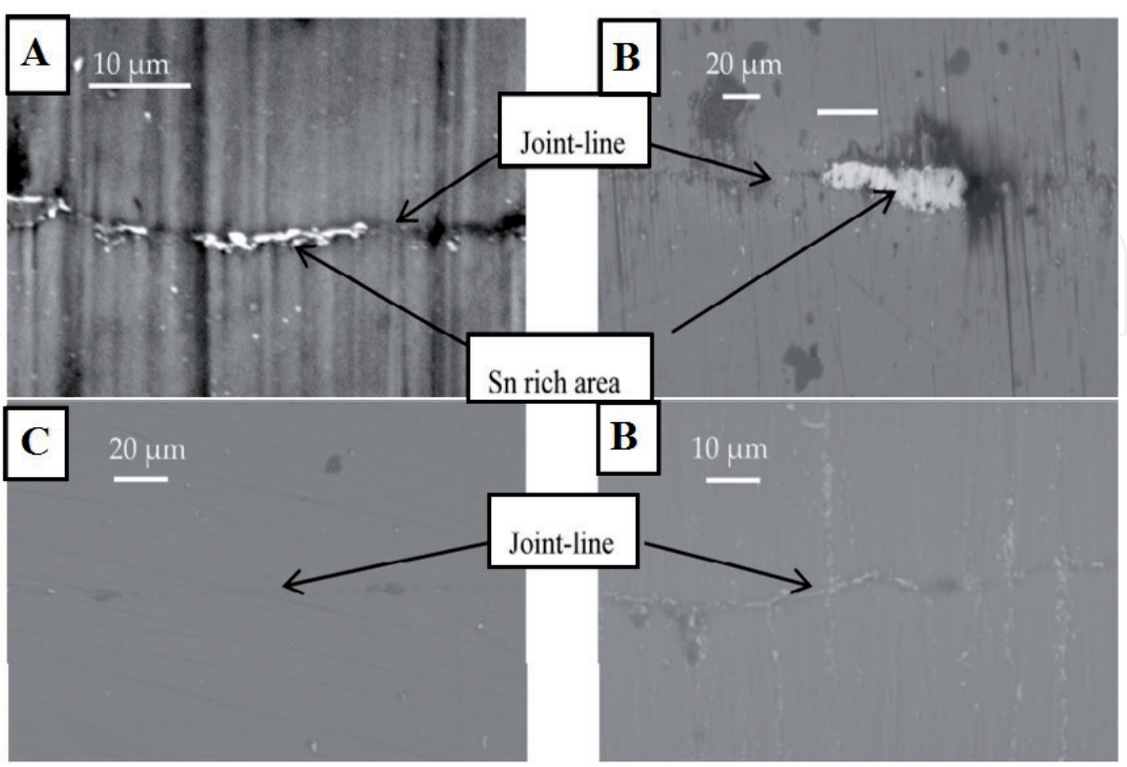


Figure 12.
SEM micrograph of region bonded using Cu-coating and Sn-foil combination as interlayers for (A) 10 minutes; (B) 20 minutes; (C) 30 minutes; and (D) 50 minutes [2].

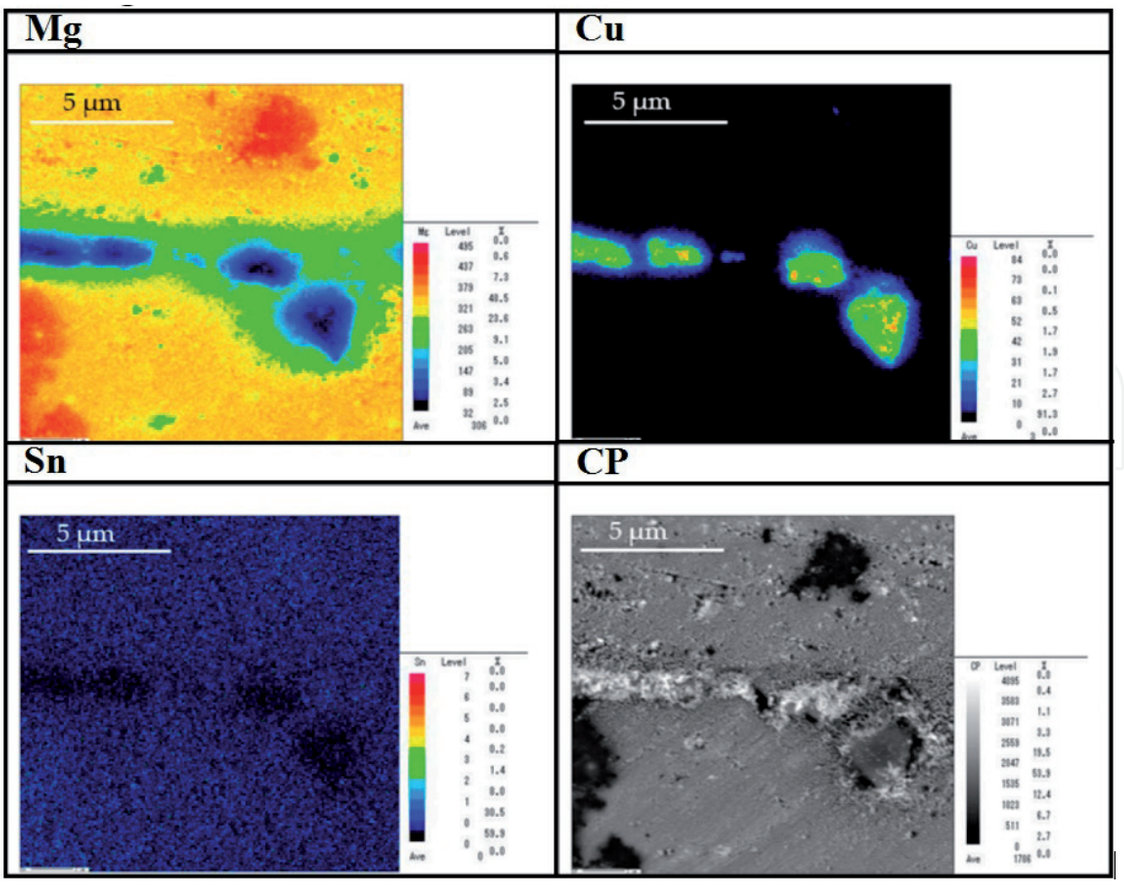


Figure 13.
Electron probe micro-analysis (EPMA) micrographs of Mg, Cu, and Sn for bonds made using Cu coating and Sn-foil interlayer at 20 minutes [2].

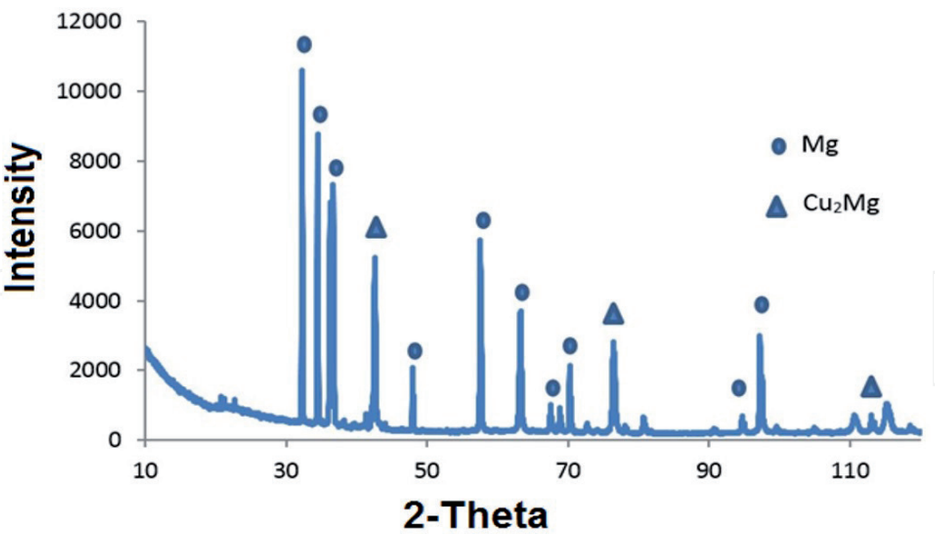


Figure 14.
XRD spectrum of the compounds formed at the interface for joint made during similar TLP bonding of Mg (AZ31) with Sn interlayer and bonded for 30 minutes.

Mg and Al using Cu/Al_2O_3 interlayer and confirms that the addition of nanoparticles can prevent the formation of a continuous IMC layer at the joint interface which leads to an increase in strength. The composition of the joint region was evaluated using EDS and is shown in **Figure 15(B)**. A summary of recent interlayers studied and the impact of composition on the mechanical performance of the bonds is presented in **Table 1**. The strength coefficient for each bond was estimated using Eq. (3).

$$m = \frac{\tau_{bond}}{\tau_b} \tag{3}$$

Where m represents the strength coefficient of the bond, τ_{bond} is the strength of the bond and τ_b is the strength of the base metal.

4.2.2 Bonding time and temperature

TLP diffusion bonding is a heavily time-dependent process with the duration of each stage contributing to the length of time required to achieve bond strength. Several models have been developed based on Fick's second law that seeks to predict the duration of each stage of the TLP bonding process. The most notable of these models was proposed by Zhou et al. [54]. Experimental research on TLP bonding of

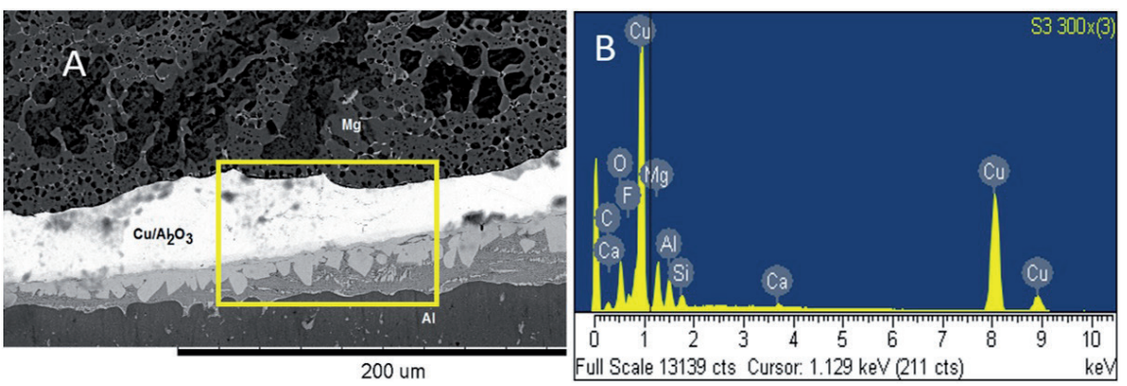


Figure 15.
(A) TLP bonding of Mg-AZ31) and Al-1100 using a Cu coating containing nano-Al_2O_3 particles and bonding condition 10 minutes at 500°C and 0.2 MPa (B) EDS analysis of the highlighted region.

Bonding system	Interlayer	Temperature (C)	Pressure (MPa)	Time (minutes)	Shear strength (MPa)	*m*	Reference
Mg-AZ31 similar bonding	Ni coatings	520	8.0	20	46.2	0.557	[49]
Mg-AZ31 similar bonding	Cu coatings	520	0.5	30	41.0	0.482	[2]
Mg-AZ31 similar bonding	Cu coatings with Sn foil	520	0.5	30	64.0	0.771	[51]
Mg AZ31	Cu foil	530	2.0	30	70.2	0.852	[3]
Mg-AZ31 and Ti-6Al-4V	Cu coatings with Sn foil	580	1.0	15	78.0	0.934	[51]
Mg-AZ31 and Ti-6Al-4V	Ni coating	540	0.2	20	50	0.602	[46]
Mg-AZ31 and Al100	Cu/Al_2O_3	500	0.2	10	20.4	0.36	Current work

Table 1.
Shear strength of diffusion bonded joints.

magnesium alloys suggests that this model is still an important tool for predicting the duration of each stage of the bonding process.

Similarly, temperature serves as an important parameter in order to produce a successful joint in the diffusion bonding as it significantly changes the kinetics of the atomic movement at the interface. Given that the interlayer melts and then solidifies at the bonding temperature and therefore, the bonding temperature should reach the melting temperature of the interlayer. The temperature used should be controlled and remain constant throughout the bonding process in order to enhance diffusion, but not cause metallurgical changes or cause excess melting of the joint region. Light metals, such as magnesium, need to be bonded at an optimal temperature so that micro-deformation is avoided.

Bonding time is a variable closely related to temperature. Increasing the bonding temperature require a shorter hold time. It is seen that increasing pressure, time and temperature produces strong joint up to a point after which the parameters become redundant. The process of diffusion bonding uses a wide range of bonding time, from seconds to hours, for different joining surfaces.

Long bonding times enhances atomic diffusion along the bond line but may increase the likelihood of IMCs forming at the interface, which are detrimental to mechanical properties. Research by Sun et al. [3] proved the influence of bonding temperature on shear and bonding strengths of the bonded joints followed by the pressure applied, holding time and surface roughness. Azizi and Alimardan [55] confirmed a direct proportion relationship existed between the increase in the width of the interface as the bonding temperature and hold time increases.

5. General remarks

The properties of magnesium alloys allow them to be used in the various structural applications including biomedical applications such as implants. Given that that magnesium is non-toxic, biocompatible and biodegradable, these materials can be used to serve as implants or replacements of body tissues. The current use of titanium implants for bone treatment and implants in the tissues may be replaced by Mg alloys since titanium alloys are not biodegradable therefore another operation/surgery is needed in most cases after the healing of the affected tissues. One direction is to develop new Mg alloys with various alloying elements such as Zn, Al, Zr, and others, in order to reach the desired degradation rate suitable for the human body. Another challenge in using Mg alloy for bone fixation is the low mechanical strength of Mg when compared to Ti.

A significant challenge, however, is identifying suitable joining technologies capable of welding/joining magnesium to other metals such as Ti and prevents IMC formations. While conventional fusion welding is also capable of a selective dissimilar joining of Mg alloys the product of these processes is not suitable for biomedical applications. On the other hand, soli-state diffusion bonding, TLP diffusion bonding process and friction stir welding have demonstrated greatest potential for the dissimilar joining of Mg alloys.

IntechOpen

Author details

Kavian O. Cooke[1,2*], Abdulaziz Alhazaa[3] and Anas M. Atieh[4]

1 School of Engineering and Informatics, University of Bradford, Bradford, UK

2 Mechanical Engineering Department, University of Technology, Jamaica WI

3 Physics and Astronomy Department, College of Science, King Saudi University, Riyadh, Saudi Arabia

4 Industrial Engineering Department, School of Applied Technical Sciences, German Jordanian University (GJU), Amman, Jordan

*Address all correspondence to: kavian_cooke@yahoo.com

IntechOpen

© 2019 The Author(s). Licensee IntechOpen. This chapter is distributed under the terms of the Creative Commons Attribution License (http://creativecommons.org/licenses/by/3.0), which permits unrestricted use, distribution, and reproduction in any medium, provided the original work is properly cited. CC BY

References

[1] Li N, Zheng Y. Novel magnesium alloys developed for biomedical application: A review. Journal of Materials Science and Technology. 2013;**29**(6):489-502

[2] Alhazaa A, Shar M, Atieh A, Nishikawa H. Transient liquid phase bonding of magnesium alloy AZ31 using Cu coatings and Cu coatings with Sn interlayers. Metals. 2018

[3] Sun DQ, Liu WH, Gu XY. Transient liquid phase bonding of magnesium alloy (Mg-3Al-1Zn) using copper interlayer. Materials Science and Technology. 2004;**20**(12):1595-1598. DOI: 10.1179/174328413X13789824293506

[4] Song G, Diao Z, Lv X, Liu L. TIG and laser-TIG hybrid filler wire welding of casting and wrought dissimilar magnesium alloy. Journal of Manufacturing Processes. 2018;**34**:204-214

[5] Peng J, Zhou C, Tao J-Q, Pan F-S. Gas tungsten arc welding of dissimilar magnesium alloys as AZ31 with AZ61. Cailiao Gongcheng/Journal of Materials Engineering. 2011;**1**(2):46-51

[6] Kurt HI, Guzelbey IH, Salman S, Asmatulu R, Dere M. Investigating the relationships between structures and properties of Al alloys incorporated with Ti and Mg inclusions. Journal of Engineering Materials and Technology. 2016;**138**(3):031006-031006-6. DOI: 10.1115/1.4032849.

[7] Liu L, Ren D. A novel weld-bonding hybrid process for joining Mg alloy and Al alloy. Materials and Design. 2011;**32**(7):3730-3735

[8] Thakur AG, Nandedkar V. Optimization of the resistance spot welding process of galvanized steel sheet using the Taguchi method. Arabian Journal for Science and Engineering. 2014;**39**(2):1171-1176

[9] Kim YG, Kim IJ, Kim JS, Il Chung Y, Choi DY. Evaluation of surface crack in resistance spot welds of Zn-coated steel. Materials Transactions. 2014;**55**(1):171-175

[10] Patel VK, Bhole SD, Chen DL. Improving weld strength of magnesium to aluminium dissimilar joints via tin interlayer during ultrasonic spot welding. Science and Technology of Welding and Joining. 2012;**17**(5):342-347. DOI: 10.1179/1362171812Y.0000000013

[11] Choi DH, Ahn BW, Lee CY, Yeon YM, Song K, Jung SB. Formation of intermetallic compounds in Al and Mg alloy interface during friction stir spot welding. Intermetallics. 2011;**19**(2):125-130

[12] Sato YS, Shiota A, Kokawa H, Okamoto K, Yang Q, Kim C. Effect of interfacial microstructure on lap shear strength of friction stir spot weld of aluminium alloy to magnesium alloy. Science and Technology of Welding and Joining. 2010;**15**(4):319-324. DOI: 10.1179/136217109X12568132624208

[13] Cooke KO, Khan TI. Resistance spot welding aluminium to magnesium using nanoparticle reinforced eutectic forming interlayers. Science and Technology of Welding and Joining. 2017;**23**(4):271-278. DOI: 10.1080/13621718.2017.1373481

[14] Penner P, Liu L, Gerlich A, Zhou Y. Feasibility study of resistance spot welding of dissimilar Al/Mg combinations with Ni based interlayers. Science and Technology of Welding and Joining. 2013;**18**(7):541-550. DOI: 10.1179/1362171813Y.0000000129

[15] Penner P, Liu L, Gerlich A, Zhou Y. Dissimilar resistance spot welding of aluminum to magnesium with Zn-coated steel interlayers. Welding Journal. 2014;**93**:225-231

[16] Xu W, Chen DL, Liu L, Mori H, Zhou Y. Microstructure and mechanical properties of weld-bonded and resistance spot welded magnesium-to-steel dissimilar joints. Materials Science and Engineering A. 2012;**537**(1):11-24

[17] Bakavos D, Prangnell PB. Mechanisms of joint and microstructure formation in high power ultrasonic spot welding 6111 aluminium automotive sheet. Materials Science and Engineering A. 2010;**527**(23):6320-6334

[18] Mordike BL, Ebert T. Magnesium properties-applications-potential. Materials Science and Engineering A. 2001;**302**(1):37-45

[19] Pareek JE, Polar M, Rumiche A, Indacochea F. Metallurgical evaluation of AZ31B-H24 magnesium alloy friction stir welds. Journal of Materials Engineering and Performance. 2007;**16**(5):655-662

[20] Feng Y, Li Y, Luo Z, Ling Z, Wang Z. Resistance spot welding of Mg to electro-galvanized steel with hot-dip galvanized steel interlayer. Journal of Materials Processing Technology. 2016;**236**:114-122

[21] Shah LH, Othman NH, Gerlich A. Review of research progress on aluminium-magnesium dissimilar friction stir welding. Science and Technology of Welding and Joining. 2018;**23**(3):256-270. DOI: 10.1080/13621718.2017.1370193

[22] Thomas WM, Nicholas ED, Needham JC, Murch MG, Temple-Smith P, Dawes CJ. Improvements Relating to Friction Welding. International Patent. December 1991. Application No. PCT/GB92/02203. Publication No. WO19930109935 A1, 6

[23] Singh K, Singh G, Singh H. Review on friction stir welding of magnesium alloys. Journal of Magnesium and Alloys. 2018;**0**:1-18

[24] Mishra RS, Ma ZY. Friction stir welding and processing_PAP_pges4-7+70. Materials Science and Engineering R. 2005;**50**(1-2):1-78

[25] Zhang H. Friction stir welding of magnesium alloys. In: Welding and Joining of Magnesium Alloys. Woodhead Publishing Series in Welding and Other Joining Technologies. Sawston, UK: Cambridge. 2010;274-305

[26] Wang K, Khan HA, Li Z, Lyu S, Li J. Micro friction stir welding of multilayer aluminum alloy sheets. Journal of Materials Processing Technology. 2018;**260**:137-145

[27] Mishraa RS, Ma ZY. Friction stir welding and processing. Materials Science and Engineering R. 2005;**50**(1-2):1-78

[28] Singh G, Singh H, Singh K. Friction stir welding of magnesium alloys: A review. Asian Review of Mechanical Engineering. 2016;**5**(1):5-8

[29] Carlone P, Astarita A, Rubino F, Pasquino N. Microstructural aspects in FSW and TIG welding of cast ZE41A magnesium alloy. Metallurgical and Materials Transactions B: Process Metallurgy and Materials Processing Science. 2016;**47**(2):1340-1346

[30] Radj BM, Senthivelan T. Analysis of mechanical properties on friction stir welded magnesium alloy by applying Taguchi Grey based approach. Materials Today: Proceedings. 2018;**5**:8025-8032

[31] Mironov S, Onuma T, Sato YS, Yoneyama S, Kokawa H. Microstructural changes during tension of friction-stir welded AZ31 magnesium alloy. Materials Characterization. 2017;**130**:1-8

[32] Mironov S, Onuma T, Sato YS, Yoneyama S, Kokawa H. Tensile behavior of friction-stir welded AZ31 magnesium alloy S. Materials Science and Engineering A. 2017;**679**:272-281

[33] Woo W, Choo H, Prime MB, Feng Z, Clausen B. Microstructure, texture and residual stress in a friction-stir-processed AZ31B magnesium alloy. Acta Materialia. 2008;**56**(8):1701-1711

[34] Yang CL, Wu CS, Lv XQ. Numerical analysis of mass transfer and material mixing in friction stir welding of aluminum/magnesium alloys. Journal of Manufacturing Processes. 2018;**32**:380-394

[35] Abdollahzadeh A, Shokuhfar A, Cabrera JM, Zhilyaev AP, Omidvar H. In-situ nanocomposite in friction stir welding of 6061-T6 aluminum alloy to AZ31 magnesium alloy. Journal of Materials Processing Technology. 2019;**263**:296-307

[36] Mohammadi J, Behnamian Y, Mostafaei A, Izadi H, Saeid T, Kokabi AH, et al. Friction stir welding joint of dissimilar materials between AZ31B magnesium and 6061 aluminum alloys: Microstructure studies and mechanical characterizations. Materials Characterization. 2015;**101**:189-207

[37] Wilden J, Jahn S, Beck W. Some examples of current diffusion bonding applications. In: Material-wissenschaft und Werkstofftechnik. 2008;**39**(4-5):349-352

[38] Maharana HS, Ashok A, Pal S, Basu A. Surface-mechanical properties of electrodeposited Cu-Al_2O_3 composite coating and effects of processing parameters. Metallurgical and Materials Transactions A, Physical Metallurgy and Materials Science. 2016;**47**(1):388-399

[39] Somekawa H, Hosokawa H, Watanabe H, Higashi K. Diffusion bonding in superplastic magnesium alloys. Materials Science and Engineering A. 2003;**339**(1-2):328-333

[40] Khoshhal R, Soltanieh M, Mirjalili M. Formation and growth of titanium aluminide layer at the surface of titanium sheets immersed in molten aluminum. Iranian Journal of Materials Science and Engineering. 2010;**7**(1):24-31

[41] Czerwinski F, editor. Precipitates of gamma-$Mg_{17}Al_{12}$ phase in Mg-Al alloys. In: Magnesium Alloys—Design, Processing and Properties. Rijeka, Croatia: Intech; 2011

[42] I. S. Effenberg G. Part 3. Landolt-Börnstein-group IV physical chemistry (numerical data and functional relationships in science and technology). In: Effenberg G, editor. Light Metal Systems Materials Science International Team MSIT® Al-Mg-Ti (Aluminium-Magnesium-Titanium). Vol 11A3, I. S. Berlin, Heidelberg: Springer; 2011

[43] Alhazaa TIKA, Haq I. Transient liquid phase (TLP) bonding of Al7075 to Ti-6Al-4V alloy. Materials Characterization. 2010;**61**:312-317

[44] Cooke KO, Khan TI, Oliver GD. Transient liquid phase diffusion bonding Al-6061 using nano-dispersed Ni coatings. Materials and Design. 2012;**33**(1)

[45] Cooke K. Spectroscopic Analyses of Nano-Dispersion Strengthened Transient Liquid Phase Bonds: In Advance aspects of Spectroscopy, Rijeka, Croatia: Intech. 2012:309-340

[46] Atieh AM, Khan TI. Effect of interlayer thickness on joint formation between Ti-6Al-4V and Mg-AZ31 alloys. Journal of Materials Engineering and Performance. 2014;**23**(11):4042-4054

[47] Cooke K, Oliver G, Buchanan V, Palmer N. Optimisation of the electric wire arc-spraying process for improved wear resistance of sugar mill roller shells. Surface and Coatings Technology. 2007;**202**(1):185-188

[48] Jin YJ, Khan TI. Effect of bonding time on microstructure and mechanical

properties of transient liquid phase bonded magnesium AZ31 alloy. Materials and Design. 2012;**38**:32-37

[49] Alhazaa AN, Khalil KA, Shar MA. Transient liquid phase bonding of magnesium alloys AZ31 using nickel coatings and high frequency induction heat sintering. Journal of King Saud University - Science. 2016;**28**(2):152-159

[50] Zhang J, Luo G, Wang Y, Shen Q, Zhang L. An investigation on diffusion bonding of aluminum and magnesium using a Ni interlayer. Materials Letters. 2012;**83**(15):189-191

[51] Alhazaa AN, AlGharbi SH, Nishikawa H. Effect of bonding temperature on the joining of Ti-6Al-4V alloy using Cu coatings and Sn interlayers. Journal of Materials Engineering and Performance. 2017;**26**(1):407-417

[52] Cooke KO. A study of the effect of nanosized particles on transient liquid phase diffusion bonding al6061 metal-matrix composite (MMC) using Ni/Al_2O_3 Nanocomposite interlayer. Metallurgical and Materials Transactions B: Process Metallurgy and Materials Processing Science. 2012;**43**(3):627-634

[53] Atieh AM, Khan TI. Application of Ni and Cu nanoparticles in transient liquid phase (TLP) bonding of Ti-6Al-4V and Mg-AZ31 alloys. Journal of Materials Science. 2014;**49**(22):7648-7658

[54] Zhou Y, Gale WF, North TH. Modelling of transient liquid phase bonding. International Materials Review. 1995;**40**(5):181-196. DOI: 10.1179/imr.1995.40.5.181

[55] Azizi A, Alimardan H. Effect of welding temperature and duration on properties of 7075 Al to AZ31B Mg diffusion bonded joint. Transactions of Nonferrous Metals Society of China. 2016;**26**(1):85-92